Partitioning technique for discrete quantum systems

L. Jin and Z. Song[*]

School of Physics, Nankai University, Tianjin 300071, China
(Received 5 January 2011; revised manuscript received 28 April 2011; published 24 June 2011)

We develop the partitioning technique for quantum discrete systems. The graph consists of several subgraphs: a central graph and several branch graphs, with each branch graph being rooted by an individual node on the central one. We show that the effective Hamiltonian on the central graph can be constructed by adding additional potentials on the branch-root nodes, which generates the same result as does the the original Hamiltonian on the entire graph. Exactly solvable models are presented to demonstrate the main points of this paper.

I. INTRODUCTION

The Schrödinger equation lies at the heart of quantum mechanics. A secular equation has analytic solutions only for a few very special cases. Approximation techniques and computational methods have been developed for treating such problems. Many of them are rooted in the partitioning technique [1,2], which was introduced by Feshbach [3] and Löwdin [4] independently. Discrete models, including quantum networks, have been a cornerstone of theoretical explorations due to their analytical and numerical tractability [5], the availability of exact solutions, and the ability to capture counterintuitive physical phenomena, such as nonspreading wave packets [6] and Bloch oscillations [7–9] in linear chains. In recent years, optical lattices [10,11], photonic crystals [12,13], etc., have increasingly permitted the experimental exploration of quantum discrete models.

In this paper, we study the partitioning technique for quantum discrete systems. The concerned graph consists of several subgraphs: a central graph and several branch graphs, with each branch graph being rooted by an individual node on the central one. Applying the projection theory [4] to such a graph, we show that the effective Hamiltonian on the central graph can be constructed by adding additional potentials on the branch-root nodes, which generates the same result as does the the original Hamiltonian on the entire graph. As the demonstration, we present two exactly solvable models, which correspond to real and imaginary potentials.

This paper is organized as follows. Section II shows a formalism for the partitioning technique in discrete quantum systems. Section III is the heart of this paper, which presents a method to obtain the projection Hamiltonian. Section IV consists of two exactly solvable examples to illustrate our main idea. Section V is the summary and discussion.

II. PARTITIONING TECHNIQUE

Löwdin has developed a partitioning technique in the algebra of matrices, with which various self-consistent field methods can be nicely formulated. In this procedure, the original Hamiltonian is simply transformed in a chosen discrete representation. The entire space is usually divided into two subspaces, a model space and an orthogonal space. The basic idea is to find an effective Hamiltonian which acts only within the target model space but generates the same result as the original Hamiltonian acting on the complete space [1,2]. The partitioning technique enables us focus our interest on a certain part of the system. In general, the effective Hamiltonian cannot be obtained explicitly, but provides a formalism to develop the perturbation method.

In the following we will show that, when the technique is applied to a specific discrete system, the effective Hamiltonian is of realistic significance. We consider a quantum graph, which is a collection of nodes and edges. It is also equivalent to a single-particle tight-binding model. For simplicity, we partition the complete graph into three subgraphs, a central part c, and two independent branches a and b. (See Fig. 1.)

The Hamiltonian (or connectivity matrix) of such a graph has the form

$$H = \begin{pmatrix} H_a & H_{ac} & 0 \\ H_{ca} & H_c & H_{cb} \\ 0 & H_{bc} & H_b \end{pmatrix}, \tag{1}$$

where

$$H_a = -\sum_{i,j=1}^{N_a} \left(\kappa_{ij}^a \, |i\rangle_a \, \langle j| + \text{H.c.} \right), \tag{2}$$

$$H_b = -\sum_{i,j=1}^{N_b} \left(\kappa_{ij}^b \, |i\rangle_b \, \langle j| + \text{H.c.} \right), \tag{3}$$

$$H_c = -\sum_{i,j=1}^{N_c} \left(\kappa_{ij}^c \, |i\rangle_c \, \langle j| + \text{H.c.} \right). \tag{4}$$

Here $N_{\gamma=a,b,c}$ denotes the dimension of the three subgraphs. $\kappa_{ij}^{\gamma=a,b,c}$ denotes the coupling between i and j of the graph γ, and reduces to the on-site potential for $i = j$. The connections between the subgraphs are

$$H_{ca} = H_{ac}^\dagger = -\sum_{i=1}^{N_c} \sum_{j=1}^{N_a} g_{ij}^a \, |i\rangle_{ca} \, \langle j|, \tag{5}$$

$$H_{cb} = H_{bc}^\dagger = -\sum_{i=1}^{N_c} \sum_{j=1}^{N_b} g_{ij}^b \, |i\rangle_{cb} \, \langle j|, \tag{6}$$

where $g_{ij}^{\gamma=a,b}$ is the coupling strength between $|j\rangle_\gamma$ and branch-root nodes $|i\rangle_c$.
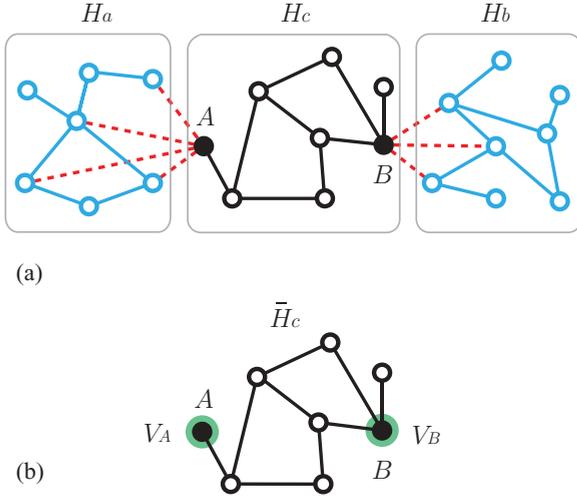
---

*songtc@nankai.edu.cn

FIG. 1. (Color online) (a) Schematic illustration of the graph consisted of two branch graphs a, b (cyan) and a center graph c (black). The dashed edges (red) represent the connections between them, with A and B being the branch-root nodes. (b) The Löwdin's projection Hamiltonian for the center graph which is composed of the original Hamiltonian H_c and additional on-site potentials V_A and V_B on nodes A and B, respectively.

Our aim is the solution of the Schrödinger equation

$$H \, |f_k\rangle = E_k \, |f_k\rangle , \tag{7}$$

where

$$|f_k\rangle = \sum_{\gamma=a,b,c} \sum_{l=1}^{N_\gamma} f_k^\gamma (l) \, |l\rangle_\gamma . \tag{8}$$

Then the Schrödinger equation can be written in the matrix form

$$\begin{pmatrix} H_a & H_{ac} & 0 \\ H_{ca} & H_c & H_{cb} \\ 0 & H_{bc} & H_b \end{pmatrix} \begin{pmatrix} f_k^a \\ f_k^c \\ f_k^b \end{pmatrix} = E_k \begin{pmatrix} f_k^a \\ f_k^c \\ f_k^b \end{pmatrix} , \tag{9}$$

and more explicit form

$$H_a f_k^a + H_{ac} f_k^c = E_k f_k^a , \tag{10}$$

$$H_c f_k^c + H_{ca} f_k^a + H_{cb} f_k^b = E_k f_k^c , \tag{11}$$

$$H_b f_k^b + H_{bc} f_k^c = E_k f_k^b . \tag{12}$$

Under the condition of the existence of the inverse matrices $(E_k - H_a)^{-1}$ and $(E_k - H_b)^{-1}$, we have

$$f_k^a = (E_k - H_a)^{-1} \, H_{ac} f_k^c , \tag{13}$$

$$f_k^b = (E_k - H_b)^{-1} \, H_{bc} f_k^c . \tag{14}$$

Then the Löwdin's projection Hamiltonian $\bar{H}_c$ has the form

$$\bar{H}_c = H_c + \bar{H}_a + \bar{H}_b , \tag{15}$$

where

$$\bar{H}_a = H_{ca}(E_k - H_a)^{-1} H_{ac} , \tag{16}$$

$$\bar{H}_b = H_{cb}(E_k - H_b)^{-1} H_{bc} . \tag{17}$$

Remarkably, the corresponding Schrödinger equation for the subgraph c [Eq. (11)] is reduced to

$$\bar{H}_c f_k^c = E_k f_k^c , \tag{18}$$

i.e., formally $\bar{H}_c$ can lead the same result as the original Hamiltonian acted with respect to the whole graph, then is referred to as the effective Hamiltonian for the central graph. Nevertheless, in general, one cannot treat Eq. (18) as usual since it is hard to obtain the explicit matrix form of $\bar{H}_c$.

III. EFFECTIVE HAMILTONIAN FOR CENTRAL GRAPH

It can be seen from Eq. (15) that $\bar{H}_c$ is constructed based on the original subgraph H_c. It indicates that the impact of two branch graphs can be projected on the target graph as additional couplings or on-site potentials. In this paper, we investigate a graph with each independent branch graph connected to the central graph c via a *single* node on the central graph. This is crucial and our conclusion is available for a graph with arbitrary branches. In the following we will show that $\bar{H}_a$ and $\bar{H}_b$ have a concise form and a clear physical meaning.

The connections between the subgraphs are

$$H_{ca} = H_{ac}^\dagger = -\sum_{j}^{N_a} g_j^a \, |A\rangle_{ca} \, \langle j| , \tag{19}$$

$$H_{cb} = H_{bc}^\dagger = -\sum_{j}^{N_b} g_j^b \, |B\rangle_{cb} \, \langle j| . \tag{20}$$

Note that there is only one branch-root node for each branch, that is, the unique restriction to the graph.

We note from Eq. (19) that the elements of H_{ca} and $H_{ac}^\dagger$ are all zeros except the row connecting to node A, i.e.,

$$H_{ca} (m,n) = \delta_{mA} g_n^a , \quad H_{ac}(m,n) = \delta_{nA} \left(g_m^a \right)^* . \tag{21}$$

Taking $M^a = (E_k - H_a)^{-1}$ and assuming its existence for the considering eigenvalue E_k, we have

$$\begin{aligned} \bar{H}_a(m,n) &= \sum_{j'=1}^{N_a} \left[\sum_{j=1}^{N_a} H_{ca}(m,j) M^a(j,j') \right] H_{ac}(j',n) \\ &= \sum_{j'=1}^{N_a} \left[\sum_{j=1}^{N_a} \delta_{mA} g_j^a M^a(j,j') \right] \delta_{nA} \left(g_{j'}^a \right)^* \\ &= \delta_{mA} \delta_{nA} \sum_{j,j'=1}^{N_a} g_j^a \left(g_{j'}^a \right)^* M^a(j,j') . \end{aligned} \tag{22}$$

Moreover, from Eqs. (13) and (16) we obtain

$$H_{ca} f_k^a = \bar{H}_a f_k^c \tag{23}$$

and its explicit form

$$\sum_{j=1}^{N_a} g_j^a f_k^a(j) = f_k^c (A) \sum_{j,j'=1}^{N_a} g_j^a \left(g_{j'}^a \right)^* M^a(j,j') . \tag{24}$$

Considering the nontrivial case $f_k^c(A) \neq 0$, the effective Hamiltonian $\bar{H}_a$ can be expressed as

$$\bar{H}_a(m,n) = \frac{\delta_{mA}\delta_{nA}}{f_k^c(A)} \sum_{j=1}^{N_a} g_j^a f_k^a(j). \tag{25}$$

By a similar procedure we obtain the expression for the effective Hamiltonian $\bar{H}_b$

$$\bar{H}_b(m,n) = \frac{\delta_{mB}\delta_{nB}}{f_k^c(B)} \sum_{j=1}^{N_b} g_j^b f_k^b(j). \tag{26}$$

Surprisingly, matrix $\bar{H}_a$ ($\bar{H}_b$) contains only one nonzero element $\bar{H}_a(A,A)$ [$\bar{H}_b(B,B)$], which can be regarded as an effective on-site potential at the branch-root node A (B). Actually, this is caused by the unique restriction. Then the physics of the projection Hamiltonian is very clear: the original target Hamiltonian with additional potentials at the joint sites. The effective potential is a weighted summation of the coupling strength $\{g_j^{\gamma=a,b}\}$ and the corresponding amplitudes $\{f_k(j)\}$. It would be noted that this conclusion can be generalized into graphs with more independent branches $d, e, \ldots$.

One can simply classify the branch graph as finite or infinite. For a finite graph without flux, we have $\{g_j^{\gamma=a,b,\ldots}\}$ and the corresponding $\{f_k(j)\}$ are all real, then the effective on-site potentials are real. In contrary, for an infinite graph, when dealing with the scattering problem, the effective on-site potentials could be complex. For a broader perspective concerning the resulting complex potentials, see the review in Ref. [14] and references therein.

IV. ILLUSTRATIVE EXAMPLES

In this section, two typical examples, which consist of finite and infinite branch graphs, are respectively investigated to exemplify the formalism developed above.

A. Finite chain

We first take a finite chain N as an example, with the Hamiltonian in the form

$$H_{\text{Chain}} = -J \sum_{i=1}^{N-1} (|i\rangle\langle i+1| + \text{H.c.}).$$

It is well known that the eigenvalue E_k and the corresponding eigenvector f_k are

$$E_k = -2J \cos k, \tag{27}$$

$$f_k(j) = \sqrt{\frac{2}{N+1}} \sin(kj), \tag{28}$$

$$k = \frac{n\pi}{N+1}, \quad n \in [1, N].$$

Now we divide the chain N as the central part N_c and two branches N_a, N_b as mentioned above. The two branch-root nodes are located at the (N_a+1)th and (N_a+N_c)th sites.

From Eqs. (25) and (26), the projection Hamiltonian can be obtained as

$$\bar{\mathcal{H}}_c = -J \sum_{i=N_a+1}^{N_a+N_c-1} (|i\rangle\langle i+1| + \text{H.c.}) + V_A|N_a+1\rangle\langle N_a+1|$$
$$+ V_B|N_a+N_c\rangle\langle N_a+N_c|, \tag{29}$$

where the on-site potentials are

$$V_A = -J \frac{\sin(kN_a)}{\sin[k(N_a+1)]}, \tag{30}$$

$$V_B = -J \frac{\sin[k(N_a+N_c+1)]}{\sin[k(N_a+N_c)]}. \tag{31}$$

In Appendix Aa, it is shown that E_k is always the eigenvalue of $\bar{\mathcal{H}}_c$ and the corresponding eigenvector of $\bar{\mathcal{H}}_c$ is in accord with that of H_{Chain} within the central chain c. It is noted that potential V_A (V_B) does not exists in the case $\sin[k(N_a+1)] = 0$ ($\sin[k(N_a+N_c)] = 0$). Actually, the corresponding eigenfunction has a vanishing amplitude at node A (B), and E_k is also the eigenvalue of the branch Hamiltonian H_a (H_b) simultaneously. From the viewpoint of the projection theory, the corresponding inverse matrix $(E_k - H_a)^{-1}$ or $(E_k - H_b)^{-1}$ does not exist.

Now we look at a concrete example in order to give a sense of the conclusion. Consider a 15-site chain with $N_a = 5$, $N_c = 4$, and $N_b = 6$. Taking $k = \pi/4$ as an example, the corresponding eigenvalues and eigenvectors for the entire chain are $E_{\pi/4} = -\sqrt{2}J$, $f_{\pi/4}(j) = (\sqrt{2}/4)\sin(j\pi/4)$, on the central chain c, $(f_{\pi/4}^c)^\dagger = -(\sqrt{2}, 1, 0, -1)/4$. On the other hand, from Eqs. (27), (28), (30), and (31), we have $V_A = -J\sin(5k)/\sin(6k) = -(\sqrt{2}/2)J$ and $V_B = -J\sin(10k)/\sin(9k) = -\sqrt{2}J$. Then the corresponding effective Hamiltonian is

$$H_c^{\text{eff}} = -J \sum_{i=6}^{8} (|i\rangle\langle i+1| + \text{H.c.}) - J\left(\frac{\sqrt{2}}{2}|6\rangle\langle 6| + \sqrt{2}|9\rangle\langle 9|\right), \tag{32}$$

and to solve H_c^{eff}, we use Eq. (A6) derived in Appendix Aa. It becomes

$$\sin(4\kappa)\left(2\cos\kappa - \frac{3\sqrt{2}}{2}\right) = 0, \tag{33}$$

which has the solutions $E_\kappa = -2J\cos\kappa = \sqrt{2}J$, 0, $-\sqrt{2}J$, and $-3\sqrt{2}/2J$. The corresponding eigenvector for $E_\kappa = -\sqrt{2}J$ can be obtained as $(f_{\pi/4}^{\text{eff}})^\dagger \propto (\sqrt{2}, 1, 0, -1)$, which is in accord with the wave function of whole system within the chain c, $f_{\pi/4}^c$.

B. Scattering problem

In the above example, we can see that all the potentials are real. It was predicted that the infinite branches could induce the imaginary potentials. Here we are interested in the scattering solution of an infinite system. Quantum scattering and transport properties in quantum networks are important features in quantum information science [6,15,16]. Now we
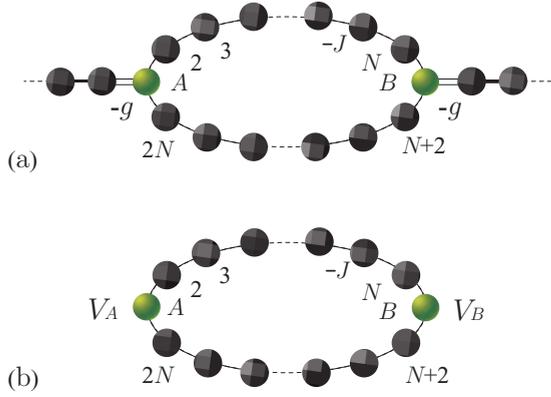
FIG. 2. (Color online) Schematic illustration of the concrete configuration for a scattering system. A ring as the scattering center connects to two semi-infinite chains L and R as waveguides with coupling $-g$. The wave function within the scattering center for a scattering state of the whole system is identical to an equal-energy eigenfunction of the projection Hamiltonian, which is constructed by the center ring with additional on-site potentials V_A and V_B added at the joint sites A and B.

consider an exactly solvable but nontrivial system to illustrate the main idea of this paper.

The graph is constructed by a uniform ring system and two semi-infinite chains as the input and output leads, which is schemed in Fig. 2. It is worthy to point out that a well-established Green's function technique [16–18] can be employed to obtain the reflection and transmission coefficients for a given incoming plane wave. The corresponding wave function within the scattering center should be obtained via the Bethe ansatz method. The Hamiltonian can be written as

$$H_s = \mathcal{H}_a + \mathcal{H}_b + \mathcal{H}_c$$
$$- \sqrt{2}J(|-1\rangle_{ac}\langle 1| + |1\rangle_{bc}\langle N+1| + \text{H.c.}), \quad (34)$$

where $\mathcal{H}_a$ ($\mathcal{H}_b$) represents a uniform input (output) waveguide as

$$\mathcal{H}_a = -J \sum_{i=-1}^{-\infty} (|i-1\rangle_a\langle i| + \text{H.c.}), \quad (35)$$

$$\mathcal{H}_b = -J \sum_{i=1}^{+\infty} (|i\rangle_b\langle i+1| + \text{H.c.}), \quad (36)$$

and the uniform ring as the scattering center is described as

$$\mathcal{H}_c = -J \sum_{i=1}^{2N} (|i\rangle_c\langle i+1| + \text{H.c.})$$
$$- V(|1\rangle_c\langle 1| + |N+1\rangle_c\langle N+1|), \quad (37)$$

where $|2N+1\rangle_c \equiv |1\rangle_c$.

There are on-site potentials V at the sites $|1\rangle_c$ and $|N+1\rangle_c$, which are the two branch-root nodes, i.e., $|A\rangle_c = |1\rangle_c$ and $|B\rangle_c = |N+1\rangle_c$. The corresponding Löwdin's projection Hamiltonian depends on the energy E_k of the incident plane wave as well as the parameter V. To be concise, as an illustrative example, we would like to present the exactly solvable model, which is helpful to demonstrate our main idea. Therefore, we will focus on this case: The incident wave

has energy $E_k = V \in (-2J, 2J)$. For such an incident plane wave, the scattering wave function can be obtained by the Bethe ansatz method. The wave function has the form

$$f_k^a(l) = e^{ik(l+1)}, \quad l \in (-\infty, -1], \quad (38)$$

$$f_k^c(l) = e^{ikl}/\sqrt{2}, \quad l \in [1, N+1], \quad (39)$$

$$f_k^b(l) = e^{ik(l+N+1)}, \quad l \in [1, \infty), \quad (40)$$

where $f_k^c(l) \equiv f_k^c(2N+2-l)$. Then the effective Hamiltonian $\bar{\mathcal{H}}_a, \bar{\mathcal{H}}_b$ can be obtained directly from Eqs. (25) and (26), which have the form

$$\bar{\mathcal{H}}_a(A, A) = -\frac{\sqrt{2}J f_k^a(-1)}{f_k^c(1)} = -2J e^{-ik}, \quad (41)$$

$$\bar{\mathcal{H}}_b(B, B) = -\frac{\sqrt{2}J f_k^b(1)}{f_k^c(N+1)} = -2J e^{ik}. \quad (42)$$

The projection Hamiltonian $\bar{\mathcal{H}}_c$ ($\bar{\mathcal{H}}_c = \mathcal{H}_c + \bar{\mathcal{H}}_a + \bar{\mathcal{H}}_b$) is

$$\bar{\mathcal{H}}_c = -J \sum_{i=1}^{2N} (|i\rangle_c\langle i+1| + |i+1\rangle_c\langle i|) + 2iJ \sin k|1\rangle_c\langle 1|$$
$$- 2iJ \sin k|N+1\rangle_c\langle N+1|. \quad (43)$$

It is a $\mathcal{PT}$-symmetric non-Hermitian Hamiltonian. Since the seminal discovery by Bender [19], it is found that the non-Hermitian Hamiltonian with simultaneous unbroken $\mathcal{PT}$ symmetry has an entirely real quantum mechanical energy spectrum and has profound theoretical and methodological implications. Many schemes aiming at a physical realization of the $\mathcal{PT}$-symmetric system in optical structures have been proposed—for example, see Ref. [20]. In Appendix A2, it is shown the spectrum $\{\varepsilon\}$ of $\bar{\mathcal{H}}_c$ consists of a band

$$\varepsilon_j = -2J \cos(j\pi/N)$$
$$(j \in [1, N-1], \text{twofold degeneracy}) \quad (44)$$

and two additional levels

$$\varepsilon_\pm = \pm V. \quad (45)$$

The eigenstates with eigenvalue ε_j can be decomposed into two kinds: symmetric and antisymmetric with respect to the spatial reflection symmetry about the axis along the waveguides. For the scattering problem, only the symmetric states are involved. It shows that among the eigenvalues, the eigenvalue $\varepsilon_+ = V$ from the spectrum $\{\varepsilon\}$ matches the energy E_k ($E_k = V$) of the incident wave. Moreover, at the end of Appendix A, it is shown that the corresponding eigenvector for ε_+ is in accord with f_k^c. Thus it is in agreement with the conclusion of the partitioning technique that there always exists a solution of the projection Hamiltonian to match the incident wave energy.

V. SUMMARY

In summary, we apply Löwdin's projection theory to the specified network, which consists of a central graph and several branch graphs. It is shown that the effective Hamiltonian on the central graph can be constructed by adding additional potentials on the branch-root nodes, which can be expressed as a weighted summation of the corresponding wave function and generates the same result as does the the original Hamiltonian

on the entire graph. It indicates that the impact of the branch graph to the central one is local and takes the role of the on-site potential. Finite and infinite exactly solvable models are presented to demonstrate our conclusion.

APPENDIX: BETHE ANSATZ SOLUTION

In this Appendix, we will derive the central formula for studying the eigenproblem of the projection Hamiltonian introduced in Sec. IV.

1. *N*-site uniform chain

We consider a uniform chain with potentials at ends. The projection Hamiltonian is

$$H_c^{\text{eff}} = -J \sum_{i=1}^{N_c-1} (|i\rangle\langle i+1| + \text{H.c.}) + V_A |1\rangle\langle 1|$$
$$+ V_B |N_c\rangle\langle N_c|, \tag{A1}$$

where V_A and V_B are defined in Eqs. (30) and (31). The Bethe ansatz eigenvector has the form

$$f_\kappa = A_\kappa e^{i\kappa j} + B_\kappa e^{-i\kappa j}, \quad j \in [1, N_c]. \tag{A2}$$

The Schrödinger equation $H_c^{\text{eff}}|f_\kappa\rangle = E_\kappa |f_\kappa\rangle$ can be written in the explicit form

$$V_A f_\kappa(1) - J f_\kappa(2) = E_\kappa f_\kappa(1),$$
$$-J f_\kappa(j-1) - J f_\kappa(j+1) = E_\kappa f_\kappa(j),$$
$$j \in [2, N_c - 1], \tag{A3}$$
$$-J f_\kappa(N_c - 1) + V_B f_\kappa(N_c) = E_\kappa f_\kappa(N_c).$$

Substituting Eq. (A2) into Eq. (A3), we obtain

$$J^2 \sin[\kappa(N_c + 1)] + J(V_A + V_B)\sin(\kappa N_c)$$
$$+ V_A V_B \sin[\kappa(N_c - 1)] = 0, \tag{A4}$$

$$E_\kappa = -2J \cos \kappa. \tag{A5}$$

Equation (A4) determines the solution of κ, while Eq. (A5) is the corresponding spectrum. Substituting Eqs. (30) and (31) into Eq. (A4), we have

$$\sin k / \{\sin[k(N_a + 1)] \sin[k(N_a + N_c)]\}$$
$$\times \{\sin[k(N_c - 1)]\sin(\kappa N_c) - \sin(k N_c)\sin[\kappa(N_c - 1)]\}$$
$$+ 2\sin(\kappa N_c)(\cos \kappa - \cos k) = 0, \tag{A6}$$

which seems difficult to solve. However, it can be simply proved by straightforward algebra that $\kappa = k$ is a solution for the equation. Accordingly, $E_\kappa = -2J\cos\kappa = -2J\cos k$ is an eigenvalue of the effective Hamiltonian of Eq. (A1). Now we try to find the corresponding eigenvector of E_κ. From Eq. (A2), the first equation of Eq. (A3), and the expression of V_A Eq. (30), we obtain

$$\frac{B_\kappa}{A_\kappa} = -e^{-2ikN_a}, \tag{A7}$$

and it indicates

$$f_\kappa(j) \propto \sin[k(N_a + j)], \tag{A8}$$

which is in accord with the eigenfunction Eq. (28) inside the central chain N_c.

2. Uniform ring as a scattering center

The projection Hamiltonian on a uniform ring is $\mathcal{PT}$ symmetric and can be expressed as

$$H_c^{\text{eff}} = -J \sum_{j=1}^{2N} (|j\rangle\langle j+1| + \text{H.c.})$$
$$+ 2iJ \sin k(|1\rangle\langle 1| - |N+1\rangle\langle N+1|), \tag{A9}$$

where $|j\rangle = |2N + j\rangle$. The parity operator $\mathcal{P}$ is defined by $\mathcal{P} : j \to N + 2 - j$ and the time-reversal operator $\mathcal{T}$ by $\mathcal{T} : i \to -i$. We note that the Hamiltonian H_c^{eff} also possesses the mirror symmetry with respect to the axis through the 1th and $(N+1)$th sites. This leads to the symmetric and antisymmetric solutions of the system. The symmetric Bethe ansatz eigenfunction f_κ has the form

$$f_\kappa(j)$$
$$= \begin{cases} A_\kappa e^{i\kappa j} + B_\kappa e^{-i\kappa j}, & j \in [1, N+1], \\ A_\kappa e^{i\kappa(2N+2-j)} + B_\kappa e^{-i\kappa(2N+2-j)}, & j \in [N+2, 2N]. \end{cases} \tag{A10}$$

Substituting the above wave function into the following Schrödinger equation

$$2i\sin k f_\kappa(1) - f_\kappa(2) - f_\kappa(2N) = E_\kappa f_\kappa(1)/J,$$
$$-f_\kappa(j-1) - f_\kappa(j+1) = E_\kappa f_\kappa(j)/J,$$
$$j \in [2, N] \cup [N+2, 2N], \tag{A11}$$
$$-f_\kappa(N) - f_\kappa(N+2) - 2i\sin k f_\kappa(N+1) = E_\kappa f_\kappa(N+1)/J,$$

after simplification, we obtain

$$\begin{pmatrix} D_- & D_+ \\ e^{i\kappa N} D_- & e^{-i\kappa N} D_+ \end{pmatrix} \begin{pmatrix} A_\kappa e^{i\kappa} \\ B_\kappa e^{-i\kappa} \end{pmatrix} = 0, \tag{A12}$$

$$E_\kappa = -2J \cos \kappa, \tag{A13}$$

where $D_\pm = \sin k \pm \sin \kappa$.

The existence of the solution requires

$$\sin(\kappa N)(\sin^2 \kappa - \sin^2 k) = 0. \tag{A14}$$

The solution is

$$\kappa = n\pi/N, \quad n \in [1, N-1], \quad \kappa = k, \pi - k. \tag{A15}$$

the corresponding eigenvalue is Eqs. (44) and (45).

Obviously, $E_\kappa = -2J\cos\kappa = -2J\cos k$ is an eigenvalue of the effective Hamiltonian Eq. (A9) and the corresponding eigenvector is

$$f_\kappa(j) = \begin{cases} e^{ikj}, & j \in [1, N+1], \\ e^{ik(2N+2-j)}, & j \in [N+2, 2N]. \end{cases} \tag{A16}$$

Therefore, the above eigenfunction f_κ is in accord with Eq. (39).

[1] I. Lindgren and J. Morrison, *Atomic Many-Body Theory* (Springer, Berlin, 1982).

[2] I. Hubač and S. Wilson, *Brillouin-Wigner Methods for Many-Body Systems* (Springer, New York, 2010).

[3] H. Feshbach, Ann. Phys. **5**, 357 (1958); **19**, 287 (1962).

[4] P.-O. Löwdin, J. Math. Phys. **3**, 969 (1962).

[5] X.-G. Wen, *Quantum Field Theory of Many-Body Systems* (Oxford University Press, New York, 2004).

[6] W. Kim, L. Covaci, and F. Marsiglio, Phys. Rev. B **74**, 205120 (2006).

[7] F. Bloch, Z. Phys. **52**, 555 (1929).

[8] C. Zener, Proc. R. Soc. A **145**, 523 (1934).

[9] T. Hartmann, F. Keck, H. J. Korsch, and S. Mossmann, New J. Phys. **6**, 2 (2004).

[10] I. Bloch, Nat. Phys. **1**, 23 (2005).

[11] D. Jaksch and P. Zoller, Ann. Phys. **315**, 52 (2005).

[12] E. Yablonovitch, T. J. Gmitter, and K. M. Leung, Phys. Rev. Lett. **67**, 2295 (1991).

[13] U. Grüning, V. Lehmann, and C. M. Engelhardt, Appl. Phys. Lett. **66**, 3254 (1995).

[14] J. G. Muga, J. P. Palao, B. Navarro, and I. L. Egusquiza, Phys. Rep. **395**, 357 (2004).

[15] L. Zhou, Z. R. Gong, Y. X. Liu, C. P. Sun, and F. Nori, Phys. Rev. Lett. **101**, 100501 (2008).

[16] L. Jin and Z. Song, Phys. Rev. A **81**, 022107 (2010).

[17] S. Datta, *Electronic Transport in Mesoscopic Systems* (Cambridge University Press, Cambridge, UK, 1995).

[18] S. Yang, Z. Song, and C. P. Sun, e-print arXiv:0912.0324v1.

[19] C. M. Bender and S. Boettcher, Phys. Rev. Lett. **80**, 5243 (1998).

[20] A. Ruschhaupt, F. Delgado, and J. G. Muga, J. Phys. A **38**, L171 (2005).